Site Preference of Ligand and Metal Substitution in Trigonal-Bipyramidal Metal Carbonyl Clusters

Piero Macchi, Davide M. Proserpio, and Angelo Sironi*

Dipartimento di Chimica Strutturale e Stereochimica Inorganica, Via Venezian 21, 20133 Milano, Italy

Received October 9, 1996[⊗]

Gimarc's topological charge stabilization rule (TCS), for addressing site preference, has been extended to the realm of metal carbonyl clusters using Allen's energy indexes (EIs) instead of charges. EIs have been computed within the extended Hückel (EH) approximation and, in order to assess an internal electronegativity scale for transition metals and to allow comparisons across the periodic table, a homogeneous set of EH parameters has been determined. EIs have been shown to behave similarly to charges on "clusters" with a rigid ligand stereochemistry like carboranes but, when one deals with metal carbonyl clusters and their intriguing ligand mobility, EIs are definitely superior to charges. EIs do address both "skeletal" and "ligand" site preferences according to the following rules of thumb: (i) more electronegative metal atoms occupy higher EI sites of the uniform reference frame (URF) (i.e. the one with the lower local electronegativity) and (ii) (nucleophilic) ligand substitution preferentially occurs on the lowest energy index site of the URF (i.e. the one with the largest electrophilic character). Previous attempts to rationalize site preference in metal clusters were mainly concerned with the relative strengths of metal−metal and metal−ligand bonds and substantially disregarded electronegativity differences between different metal atoms. In contrast, we have shown that the latter are important whenever the actual URF allows for different EIs on different metal sites. In particular, differences in electronegativity have been shown to be important for M_5L_{15} and M_5L_{14} but not for M_5L_{12} bipyramidal metal carbonyl clusters.

Cluster chemistry has grown in the last 30 years as a major new area of inorganic chemistry, the basic "rules" of which are now well understood, are described in dedicated textbooks,[1] and are normally part of any serious inorganic chemistry curriculum. However, even in the "old" field of metal carbonyl clusters, there are still questions which elude simple laws or rules and are difficult to answer in a general way. For instance, despite a substantial knowledge of the relationships between the shape of the metal cage and the stoichiometry of the cluster (the so-called electron counting rules), a simple working theory of ligand stereochemistry is lacking (because of the softness and smoothness of potential energy surfaces with respect to ligand mobility). Accordingly, we can foresee with paper and pencil the stoichiometry of a metal carbonyl cluster (given the shape of the metal cage) but not its ligand stereochemistry. In comparison with main-group compounds, metal carbonyl clusters have the correspondent of the *octet rule* but lack that of the *valence shell electron pair repulsion* theory.

Although numerous studies have been carried out and numerous models have been proposed to address the above structural aspects of metal carbonyl clusters, less attention has been paid to the site preference of metal atoms in mixed-metal clusters and to the site preference of ligand substitution. In order to deal with such problems, which are particularly relevant to the modeling of the catalytic behavior of clusters, we will focus our attention on another simple rule developed by Gimarc[2,3] in the area of main-group compounds, namely the *topological charge stabilization* (TCS) rule, and we will attempt its extension to the cluster realm.

Given that the pattern of charge densities in a molecule is determined, at least in part, by the topology of the molecule and the number of electrons occupying the molecular orbital system, the TCS rule says that nature prefers to locate heteroatoms, according to their electronegativity, at those positions in a molecular structure where electron density is accumulated or depleted in an isoelectronic, isostructural, homoatomic system which is called the *uniform reference frame* (URF). Theoretically, these preferences have been interpreted using first-order perturbation theory arguments.[4] Within the Hückel approximation, the change in total π-energy of a homoconjugated molecule due to the substitution of a carbon k by a heteroatom is

$$\delta E = q_k \delta\alpha + 2\sum_{1} p_{kl}\delta\beta_{kl} \qquad (1)$$

where q_k is the π-electron density of the kth atom, p_{kl} is the Mulliken bond order between the kth and lth atoms (in the URF), and $\delta\alpha$ and $\delta\beta$ are the changes of Coulomb and resonance integrals upon heteroatom substitution. Obviously, the TCS rule becomes effective whenever the electronegativity changes are significant and the stabilization energy essentially reduces to $\delta E = q_k\delta\alpha$. An example from carborane chemistry concerns

* To whom correspondence should be addressed. Email: angelo@csmtbo.mi.cnr.it.

[⊗] Abstract published in *Advance ACS Abstracts,* March 1, 1997.

(1) Mingos, D. M. P.; Wales, D. J. *Introduction to Cluster Chemistry*; Prentice-Hall: London, 1990.
(2) Gimarc, B. M. *J. Am. Chem. Soc.* **1983**, *105*, 1979.
(3) Ott, J. J.; Gimarc, B. M. *J. Am. Chem. Soc.* **1986**, *108*, 4303.
(4) Mingos, D. M. P.; Zhenyang, L. *Comments Inorg. Chem.* **1989**, *9*, 95.

S0276-7333(96)00854-0 CCC: $14.00

the relative stability of the three possible isomers of $C_2B_3H_5$. Extended Hückel computations on the trigonal-bipyramidal URF $[B_5H_5]^{2-}$, which itself has never been prepared, show the normalized charges to be negative at the apical positions and positive at the equatorial sites. Therefore, the three possible isomeric carboranes should follow the decreasing order of stability: 1,5- > 1,2- > 2,3-$C_2B_3H_5$. Given that the 1,5-isomer has a perfect match between the negative charges in the reference frame and the location of the more electronegative heteroatoms, the 1,2-isomer complies in only one of the two positions, while in the 2,3-isomer neither carbon occupies a site of greater electron density. The predicted order or stabilization agrees with what is known experimentally: the 1,5-isomer is the only known unsubstituted isomer, the 1,2-isomer exists only as the methyl-substituted form, and the 2,3-isomer has not been reported in any form. If a rule of such a predictive capability were developed for metal clusters, it would be possible, *inter alia*, to attempt a rationalization of the activities of bimetallic or multimetallic catalysts.

The first attempt to bring Gimarc's formalism into the cluster realm was made by Mingos and Zhenyang,[4] who, however, suggested that electronegativity differences, between adjacent transition metals in the periodic table, are small ($\delta\alpha \approx 0$) and that the dominant term in the stabilization energy becomes $\delta E = 2\sum_l p_{kl}\delta\beta_{kl}$. In this situation site preference depends on the different bonding capabilities of different metals, that is on the relative strengths of metal−metal and metal−ligand bonds for different atoms, which can be evaluated qualitatively from the different sizes of valence orbitals on moving from left to right and from lower to higher row atoms.

In this paper we propose, in order to generalize the Gimarc and Mingos approach, to use EH for evaluating Mulliken's atomic charges and Allen's atomic Energy Index (EI). We will focus our attention on trigonal-bipyramidal metal carbonyl clusters with a number of ligands ranging from 12 to 15 and with 72 or 76 CVE's. The complete class of molecules studied is reported in Table 1, while their structures are represented in Figure 1.

This aim can be achieved only if a homogeneous set of parameters is used for the transition metals in order to allow comparisons of numerical results on moving from left to right and from top to bottom in the periodic table. A careful examination of the literature showed that the available parameters were derived from quite different compounds, and their use could bias our results. We decided to compute a homogeneous set of parameters modeled from existing homometallic molecules with only carbonyl ligands, a formal oxidation state of the metal equal to zero, and the same structures within the same periodic group.

Table 1. Overall View of the Class of Compounds with Known Bipyramidal Structures Examined in This Work

compd	structural type	notes	CVE	ref
	M_5L_{15}			
$[Rh_5(CO)_{15}]^-$	**A** (C_2)		76	5
$[Rh_4Co(CO)_{15}]^-$	**A**	Co(3)	76	6
$[Rh_4Ir(CO)_{15}]^-$	**A**	Ir(1) 70%, Ir(3) 30%	76	6
$[Rh_3Ir_2(CO)_{15}]^-$	**A**	Ir(1), Ir(3)	76	6
$[Ir_4Fe(CO)_{15}]^{2-}$	**B** (C_s)	Fe(3)	76	7
$[Rh_4Fe(CO)_{15}]^{2-}$	**B** (C_s)	Fe(3)	76	6
$[Ir_4Ru(CO)_{15}]^{2-}$	**B** (C_s)	Ru(3)	76	8
$[Rh_4Os(CO)_{15}]^{2-}$	**B** (C_s)	Os(3)	76	9
$[Rh_4Ru(CO)_{15}]^{2-}$	**B** (C_s)	Ru(3)	76	10
$[Rh_5(CO)_{14}(SCN)]^{2-}$	**B**	SCN (3X)	76	11
$[Rh_5(CO)_{14}(CH_2CN)]^{2-}$	**B**	CH_2CN (3X)	76	12
$[Rh_5(CO)_{14}I]^{2-}$	**B**	I (3X)	76	13
$[Rh_5(CO)_{14}(PPh_3)]^-$	**B** (C_s)	PPh_3 (3Y)	76	11
$[Rh_4Ir(CO)_{14}(PPh_3)]^-$	**B** (C_s)	Ir(3), PPh_3 (3Y)	76	6
	M_5L_{14}			
$[Ir_4Pt(CO)_{14}]^{2-}$	**C** (C_2)	Pt(1)	76	14
$[Rh_4Pt(CO)_{14}]^{2-}$	**C** (C_2)	Pt(1)	76	15
$[Fe_2Ir_3(CO)_{14}]^-$	**C′** (C_2)	Fe(3), Fe(3′)	72	7
$[Ir_2Ru_3(CO)_{14}]^{2-}$	**C′** (C_2)	Ir(2), Ir(2′)	72	16
$[ReIr_4(CO)_{12}(PPh_3)_2]^-$	**D**	Re(4), PPh_3(2), PPh_3(3)	72	16
	M_5L_{12}			
$[Rh_4Pt(CO)_{12}]^{2-}$	**E** (C_s)	Pt(3)	72	15
$[Ir_4Pt(CO)_{12}]^{2-}$	**E′** (C_s)	Pt(3)	72	14

Evaluation of a Homogeneous Set of EH Parameters for Group 6−10 Transition-Metal Atoms

All the computations were of extended Hückel type with weighted Wolfsberg−Helmholz formula as implemented in CACAO[17] version 4.0 for PC and in a local modification of the code to include EIs (see below). We idealized each geometry, with minor changes in the experimental coordinates, to obtain the most common point group symmetry for the molecules of the same periodic group. For this reason we impose an ideal D_{3h} symmetry for $Fe_3(CO)_{12}$ and C_{3v} for $Ir_4(CO)_{12}$ (here, the final parameters have been averaged over the four sites). There are no isostructural carbonyl clusters for the elements of group 10, so we were forced to select a tetranuclear Pd cluster and to idealize the trinuclear Ni and Pt clusters from the observed stacked derivatives. The complete list of reference compounds is reported in Table 2.[18]

(5) Fumagalli, A.; Koezle, T. F.; Takusagawa, F.; Chini, P.; Martinengo, S.; Heaton, B. T. *J. Am. Chem. Soc.* **1980**, *102*, 1740.
(6) Moret, M. Ph.D. Thesis, University of Milan, 1991.
(7) Pergola, R. D.; Garlaschelli, L.; Demartin, F.; Manassero, M.; Masciocchi, N.; Sansoni, M.; Fumagalli, A. *J. Chem. Soc., Dalton Trans.* **1989**, 1109.
(8) Fumagalli, A.; Koezle, T. F.; Takusagawa, F.; Chini, P.; Martinengo, S.; Heaton, B. T.; Longoni, G. *Am. Cryst. Assoc., Ser. 2* **1980**, *7*, 16.
(9) Fumagalli, A.; Della Pergola, R.; Garlaschelli, L. *J. Organomet. Chem.* **1989**, *197*, 362.
(10) Fumagalli, A.; Ciani, G. *J. Organomet. Chem.* **1984**, *272*, 91.
(11) Fumagalli, A.; Martinengo, S.; Galli, D.; Allevi, C.; Ciani, G.; Sironi, A. *Inorg. Chem.* **1990**, *29*, 1408.
(12) Ragaini, F.; Porta, F.; Fumagalli, A.; Demartin, F. *Organometallics* **1991**, *10*, 3785.
(13) Evans, J.; Stroud, P. M.; Webster, M. *J. Chem. Soc., Chem. Commun.* **1991**, 1059.
(14) Fumagalli, A.; Pergola, R. D.; Bonacina, F.; Garlaschelli, L.; Moret, M.; Sironi, A. *J. Am. Chem. Soc.* **1989**, *111*, 165.
(15) Fumagalli, A.; Martinengo, S.; Chini, P.; Galli, D.; Heaton, B. T.; Della Pergola, R. *Inorg. Chem.* **1984**, *23*, 7648.
(16) Sironi, A.; *et al.* To be submitted for publication.
(17) Mealli, C.; Proserpio, D. M. *J. Chem. Educ.* **1990**, *67*, 399.
(18) Albright, T. A.; Halevi, E. A. *Aust. J. Chem.* **1993**, *46*, 259.
(19) Myers, C. E.; Norman, L. J.; Loew, L. M. *Inorg. Chem.* **1978**, *17*, 1581.
(20) Whitaker, A.; Jeffery, J. W. *Acta Crystallogr.* **1967**, *23*, 977.
(21) Munita, R.; Letelier, J. R. *Theor. Chim. Acta* **1981**, *58*, 167.
(22) Baranovskii, V. I.; Nicolskii, A. B. *Teor. Eksp. Khim.* **1967**, *3*, 527.
(23) Mak, T. C. M. *Z. Kristallogr.* **1984**, *166*, 277.
(24) Jostes, R. *Theor. Chim. Acta* **1988**, *74*, 229.

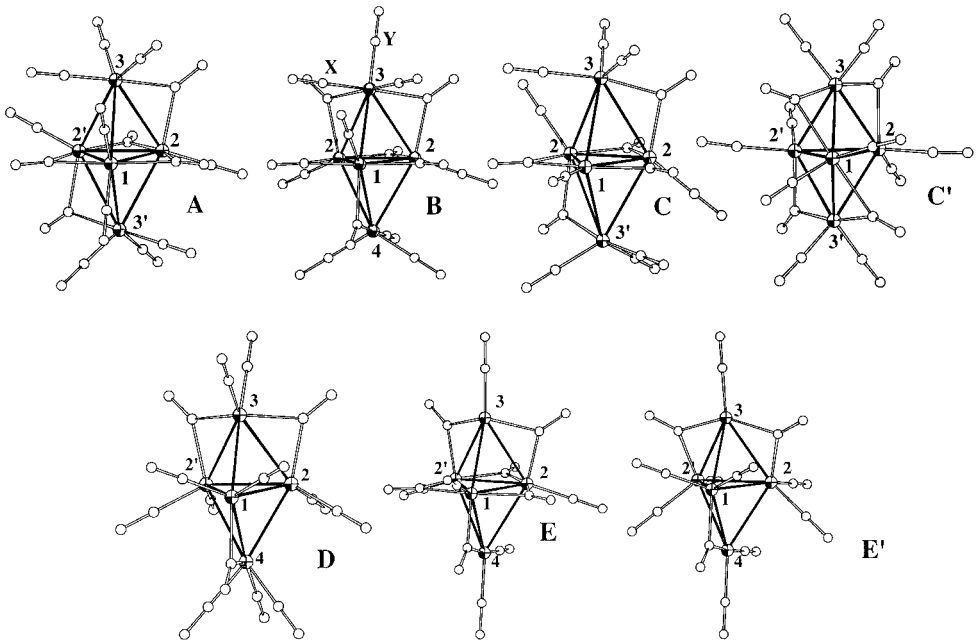

Figure 1. Representations of the trigonal-bipyramidal metal carbonyl clusters studied. See Table 1 for the labeling.

Table 2. Model Compounds Used for the Computation of H_{ii}, with References to the Charge Iteration (CI) Parameters and to the Crystal Structures

ref molecule	sym	ref for CI	ref for structure
$Cr(CO)_6$	O_h	19	20
$Mo(CO)_6$	O_h	21, 22	23
$W(CO)_6$	O_h	21, 24	25
$Mn_2(CO)_{10}$	D_{4d}	19	26
$Tc_2(CO)_{10}$	D_{4d}	21, 22	27
$Re_2(CO)_{10}$	D_{4d}	21, 24, 28	29
$Fe_3(CO)_{12}$	D_{3h}	19	30
$Ru_3(CO)_{12}$	D_{3h}	21, 22	31
$Os_3(CO)_{12}$	D_{3h}	21, 24, 28	32
$Co_4(CO)_{12}$	C_{3v}	19	33
$Rh_4(CO)_{12}$	C_{3v}	21, 22	33
$Ir_4(CO)_{12}$	C_{3v}	21, 24, 28	34
$Ni_3(CO)_6$	D_{3h}	19	35
$Pd_4(CO)_6(PH_3)_4$	T_d	21, 22	36
$Pt_3(CO)_6$	D_{3h}	21, 24, 37	35

The STO basis set (with single-ζ exponent for s and p and double-ζ exponent for d atomic orbitals) used for the elements of the second- and third-row transitions were taken from Basch and Gray.[38−40] The exponents available from Richardson *et al.*[41,42] for the elements of the first transition were already examined by Summerville and Hoffmann,[43] and they noticed that the s and p AOs were too diffuse, giving unrealistic negative reduced overlap populations for metal dimers. They introduced a new *ad hoc* set of single-ζ exponents for the s and p AOs, keeping the original double-ζ for d AOs. The scaling used results in equal values for s and p exponents for each metal. This is in disagreement with the s and p values for the second and third rows, where the ζ value for p AOs is always smaller by ∼15% than that for s AOs; moreover, plots of the s and p exponents *vs* group number showed that the parameters for second- and third-row elements run parallel, while that for first-row elements has a different slope. There are no reasons to break the periodicity observed for the higher transitions, and also this behavior is in disagreement with the same plots obtained with the exponents computed by Fitzpatrick and Murphy for single-ζ STO.[44] This latter set of parameters is not suitable for our reference molecules, giving unrealistic metal−metal reduced overlap populations: the values of the exponents are all too small by a factor of ∼0.55 when comparing second- and third-row elements. From this result we scaled the first-row ζ exponents proportionally to obtain the same first/second and first/third *ratios* observed in the set by Fitzpatrick and Murphy.[44]

With the homogeneous set of molecules and exponents for the AOs, we computed the H_{ii} values for the metals with the charge iteration parameters (CI) available in the literature and extrapolated from experimental spectroscopic data using the extended Hückel approximation with self-consistent charge and configuration procedure (SCCC) as implemented in the program

(25) Heinemann, F.; Schmidt, H.; Peters, K.; Thiery, D. *Z. Kristallogr.* **1992**, *198*, 123.
(26) Martin, M.; Rees, B.; Mitschler, A. *Acta Crystallogr.* **1982**, *B38*, 6.
(27) Bailey, M. F.; Dahl, L. F. *Inorg. Chem.* **1965**, *4*, 1140.
(28) Charkin, O. P. *Russ. J. Inorg. Chem. (Engl. Transl.)* **1974**, *19*, 1589.
(29) Churchill, M. R.; Amoh, K. N.; Wasserman, H. J. *Inorg. Chem.* **1981**, *20*, 1609.
(30) Cotton, F. A.; Troup, J. M. *J. Am. Chem. Soc.* **1974**, *96*, 4155.
(31) Churchill, M. R.; Hollander, F. J.; Hutchinson, J. P. *Inorg. Chem.* **1977**, *16*, 2655.
(32) Churchill, M. R.; Deboer, B. G. *Inorg. Chem.* **1977**, *16*, 878.
(33) Wei, C. H. *Inorg. Chem.* **1969**, *8*, 2384.
(34) Churchill, M. R.; Hutchinson, J. P. *Inorg. Chem.* **1978**, *17*, 3528.
(35) Calabrese, J. C.; Dahl, L. F.; Chini, P.; Longoni, G.; Martinengo, S. *J. Am. Chem. Soc.* **1974**, *96*, 2614.
(36) Dubrawsky, J.; Kriege-Simosden, J. C.; Felthan, R. D. *J. Am. Chem. Soc.* **1980**, *102*, 2089.
(37) Brown, D. A.; Owens, A. *Inorg. Chim. Acta* **1971**, *5*, 675.
(38) Basch, H.; Viste, A.; Gray, H. B. *Theor. Chim. Acta* **1965**, *3*, 458.
(39) Basch, H.; Gray, H. B. *Theor. Chim. Acta* **1966**, *4*, 367.
(40) Basch, H.; Viste, A.; Gray, H. B. *J. Chem. Phys.* **1966**, *44*, 10.
(41) Richardson, J. W.; Nieupoort, W. C.; Powell, R. R.; Edgell, W. F. *J. Chem. Phys.* **1962**, *36*, 1057.
(42) Richardson, J. W.; Powell, R. R.; Nieupoort, W. C. *J. Chem. Phys.* **1963**, *38*, 796.
(43) Summerville, R. H.; Hoffmann, R. *J. Am. Chem. Soc.* **1976**, *98*, 7240.
(44) Fitzpatrick, J.; Murphy *Inorg. Chim. Acta* **1984**, *87*, 41.
(45) Calzaferri, G.; Brandle, M. QCMP No. 116. *QCPE Bull.* **1992**, *12*(4), update May 1993.

Table 3. Atomic Parameters Used in the Calculations and Derived from the Molecules Reported in Table 1

	n_s[a]	ζ_s	H_{ss}	n_p[a]	ζ_p	H_{pp}	n_d[a]	H_{dd}	ζ_{1d}	ζ_{2d}	C_1	C_2	χ_s[b]	χ_{EH}[c]
Cr	4	1.773	−8.97	4	1.460	−4.54	3	−10.45	4.950	1.800	0.5058	0.6747	−8.6	−9.41
Mn	4	1.832	−9.28	4	1.526	−4.56	3	−11.24	5.150	1.900	0.5311	0.6479	−9.2	−10.24
Fe	4	1.895	−9.60	4	1.592	−4.62	3	−12.08	5.350	1.800	0.5366	0.6678	−9.9	−11.11
Co	4	1.956	−9.60	4	1.658	−4.57	3	−12.58	5.550	2.100	0.5679	0.6059	−10.4	−11.71
Ni	4	2.011	−9.62	4	1.724	−4.64	3	−13.11	5.750	2.000	0.5683	0.6292	−11.0	−12.21
Mo	5	1.960	−8.75	5	1.900	−4.62	4	−10.36	4.540	1.900	0.5899	0.5899	−8.2	−9.31
Tc	5	2.018	−9.20	5	1.984	−4.51	4	−11.25	4.900	2.094	0.5715	0.6012	−9.0	−10.23
Ru	5	2.078	−8.87	5	2.043	−4.25	4	−11.91	5.378	2.303	0.5340	0.6365	−9.8	−10.91
Rh	5	2.135	−8.79	5	2.100	−4.00	4	−12.52	5.542	2.398	0.5563	0.6119	−10.6	−11.61
Pd	5	2.190	−9.01	5	2.152	−3.25	4	−13.04	5.983	2.613	0.5264	0.6373	−11.3	−12.25
W	6	2.341	−9.93	6	2.309	−5.18	5	−10.25	4.982	2.068	0.6685	0.5424		−9.32
Re	6	2.398	−10.75	6	2.372	−5.19	5	−11.13	5.343	2.277	0.6377	0.5658		−10.19
Os	6	2.452	−10.78	6	2.429	−5.29	5	−12.08	5.571	2.416	0.6372	0.5598		−11.08
Ir	6	2.500	−10.69	6	2.484	−5.08	5	−12.73	5.796	2.557	0.6351	0.5556		−11.77
Pt	6	2.554	−10.37	6	2.554	−5.05	5	−12.96	6.013	2.696	0.6334	0.5513		−12.22

[a] n_i = principal quantum number of the atomic orbital i. [b] As reported by Allen.[53] [c] Computed from EH parameters and calculated atomic occupancies.

ICONC.[45] This procedure gives small charges on the metals, in good agreement with their formal zero oxidation state, and positive (bonding) metal−metal reduced overlap populations. When more than one set of CI parameters was available, the final H_{ii} values were the averages of those obtained (not much difference among them was observed).[46] The complete list of parameters is reported in Table 3.

To analyze site preference, previous studies identified several parameters to be used, such as metal−metal and metal−ligand bond strength, atomic charges, and overlap populations as derived from Mulliken analysis. In the search of a new quantitative index, we considered the recent electronegativity scale introduced by Allen.[47−53] The spectroscopic electronegativity (or the energy configuration of the valence state) χ_S as defined in (2) is calculated from tabulated experimental spectroscopic data, where n_s, n_p, and n_d are the atomic orbital occupancies and E_s, E_p, and E_d are their ionization potentials.

$$\chi_S = \frac{n_d \cdot E_d + n_p \cdot E_p + n_s \cdot E_s}{n_s + n_p + n_d} \qquad (2)$$

We can easily transform (2) to be used within EH, substituting the $E_{s,p,d}$ value of each valence orbital with the corresponding H_{ii} value for a given configuration. A comparison of χ_S values reported by Allen for the first and second transition series with the ones computed by us for s^2d^{n-2} configurations with $n_s = 2$, $n_p = 0$, and $n_d = n - 2$ showed that the EH values are more negative by ∼1 eV but they decrease parallel to the χ_S value, and analogously the change along a group is small (maximum 0.2 eV). We can also compute χ_{EH} (as reported in Table 3) for the configuration obtained from the Mulliken population analysis of the reference molecules used to obtain the H_{ii} values. These new values are more related to the type of molecule and show the same decrease along the period and a narrower distribution of values along the groups, confirming that it is not possible to distinguish metals of the same group on the basis of Allen electronegativity. Plots of this identical trend are shown in Figure 2.

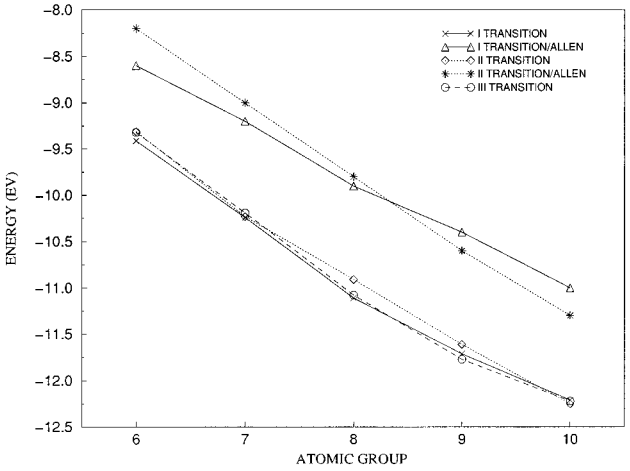

Figure 2. Comparison of χ_{EH} values calculated from EH parameters (for the three transitions) and χ_S values as reported by Allen (for the first and second rows).[53] See Table 3 for the actual values.

Allen also proposed an extension of χ_S to the molecular case, introducing the atomic energy Index (EI)

$$EI_A = \frac{\sum_i^N n_{Ai}\epsilon_i}{\sum_i^N n_{Ai}} = \frac{\sum_i^N n_i\epsilon_i \sum_j^{M(A)} \sum_k^M c_{ij}^* c_{ik} S_{jk}}{\sum_i^N n_i \sum_j^{M(A)} \sum_k^M c_{ij}^* c_{ik} S_{jk}} \qquad (3)$$

an energy-weighted population analysis that correlates with χ_S for the separated atoms (N is the total number of molecular orbitals, n_i its occupation, ϵ_i its energy, and n_{Ai} the fraction of n_i belonging to atom A; M is the total number of atomic orbitals, M(A) denotes the orbitals of atom A, c_{ij} and c_{ik} are the coefficients of the molecular orbitals, and S_{jk} is the overlap between atomic orbitals j and k). EI is the atomic average monoelectronic energy in a molecule, and the sum of all the EI_A values gives the total energy as expressed in the extended Hückel approach. This local quantity allows comparison be-

(46) The complete sets of CI parameters are available upon request from the authors. Another set of CI parameters was found in the literature: Nogueira, R. S.; Guenzburger, D. *Phys. Rev. A* **1991**, *44*, 5558. We checked it against our results and found no significant differences.

(47) Allen, L. C. *J. Am. Chem. Soc.* **1989**, *111*, 9003.
(48) Allen, L. C.; Egolf, D. A.; Knight, E. T.; Liang, C. *J. Chem. Phys.* **1990**, *94*, 5602.
(49) Allen, L. C. *Acc. Chem. Res.* **1990**, *23*, 176.
(50) Allen, L. C. *Croat. Chem. Acta* **1991**, *64*, 389.
(51) Allen, L. C.; Knight, E. T. *J. Mol. Struct. (THEOCHEM)* **1992**, *261*, 313.
(52) Allen, L. C. *Can. J. Chem.* **1992**, *70*, 31.
(53) Allen, L. C. *Int. J. Quantum Chem.* **1994**, *49*, 253.

Table 4. Energy Indexes and Atomic Charges (in Parentheses) for the Topologically Nonequivalent Metal Atoms of $[M_5(CO)_{15}]^-$ Trigonal-Bipyramidal Clusters of A (C_2) and B (C_s) Stereochemistries with Four Different Distortions of the Bridging Carbonyls[a]

M(1)−C vs M(2)−C M(2)−C vs M(3)−C	$d_5 > d_2$ $d_1 < d_3$	$d_4 = d_4$ $d_1 < d_3$	$d_4 = d_4$ $d_4 = d_4$	$d_2 < d_5$ $d_1 < d_3$
		Structure **A**		
M(1)	*−13.28 (−0.03)*	−13.36 (0.09)	−13.36 (0.12)	−13.40 (0.15)
M(2)	*−13.19 (−0.28)*	−13.17 (−0.30)	−13.18 (−0.29)	−13.13 (−0.37)
M(3)	***−13.47 (0.03)***	**−13.47 (0.03)**	**−13.46 (0.01)**	**−13.47 (0.03)**
		Structure **B**		
M(1)	−13.08 (−0.45)	−13.16 (−0.34)	−13.16 (−0.42)	*−13.23 (0.21)*
M(2)	−13.20 (−0.24)	−13.18 (−0.27)	−13.19 (−0.27)	*−13.17 (−0.29)*
M(3)	**−13.40 (0.51)**	**−13.40 (0.52)**	**−13.63 (0.56)**	***−13.41 (0.51)***
M(4)	−13.22 (−0.05)	−13.22 (−0.06)	−13.43 (0.10)	*−13.22 (−0.06)*

[a] d_1, d_2, d_3, d_4, and d_5 assume the values of 2.05, 2.08, 2.10, 2.10, and 2.22 Å for **A** and 1.98, 2.16, 2.10, and 2.10 Å for **B**. Note that M(3) has the lowest EI (but not always the highest charge), whatever the semibridging degree of the carbonyl ligands in both cases. EIs in italics refer to the two observed stereochemistries (namely **A** and **B** in Figure 1).

tween the same kinds of atoms in a molecule; that with the lowest (*most negative*) EI is the most electronegative.

Cluster URF and the Usage of Energy Indexes

Gimarc's approach cannot be directly transferred to metal carbonyl clusters. As a matter of fact, ligand mobility hampers a simple definition of the URF and the charge criterion becomes difficult to apply because the actual ligand stereochemistry of a metal cluster is normally associated with an almost uniform spread of charges on the metal atoms. Indeed, at variance from what happens in the carborane realm, substituted and parent cluster species do not normally share the same ligand connectivity pattern. Moreover, as shown in Table 4, for M_5L_{15} derivatives of C_2 and C_s symmetries, even slight perturbations on the semibridging character of bridging carbonyl ligands strongly affect the distribution of charges. In contrast, an inspection of Table 4 clearly shows that Allen's energy indexes are less dependent on details in the ligand stereochemistry and should be used instead of charges to address the proper substitution site.

Note that when charges are computed for the homoleptic $[M_n(CO)_m]^{q-}$ cluster with the ligand stereochemistry of the substituted homologue, charges always address the correct substitution site. However, we think that the *a priori* assumption of the correct final stereochemistry is too strong and cannot be made if we look for real predictions, since it applies a bias toward the correct answer.

Given the above considerations, we propose (i) to use as uniform reference frame (URF), for each M_nL_m class, the homoleptic $[M_n(CO)_m]^{q-}$ cluster with *its* idealized experimental geometry, (ii) to use energy indexes (EI) to address site preferences, (iii) that more electronegative metal atoms will occupy higher energy index sites of the URF (i.e., that with the lower local electronegativity), (iv) that, whenever the substituting metal has almost the same electronegativity as the metal of the URF (belonging to the same group of the periodic table), EI cannot discriminate between the different sites and Mingos' criterion of maximum bonding (M−M plus M−L) must be applied, and (v) that (nucleophilic) ligand substitution preferentially will occur on the lowest energy index site of the URF (i.e., that with the largest electrophilic character).

EIs deliver information about the *intrinsic* topological differences of each site *before* metal or ligand substitution. *Upon* metal or ligand substitution the ligand stereochemistry may change, but we assume that the most stable stereoisomer is always obtained for the substitutional pattern suggested by the EIs; that is, we consider these *stereochemical changes* as high-order perturbations not affecting site preference. Note, however, that the *actual stereochemistry* of the URF is very important, since sites differing only in the M−L connectivity may have different EIs and then different substitutional behavior.

We do not have any analytical or even perturbational proof for the ability of energy indexes to address site preference; however, as shown by Allen,[47,53] they correlate with charges, the larger (more positive) the charge (Q) the lower the energy index, and hence they should replicate charge performances. However, we have seen that charges cannot be used for clusters and we have still to understand why EIs could. A possible explanation lies in the different slopes of the Q/EI correlation for soft and hard atoms. As shown by Allen,[47,53] the harder the atom, the lower the slope. Hence, for transition-metal atoms, which are rather soft, large charge variations afford moderate changes in the EI and ligand mobility grants for charge equalization without substantially altering the "intrinsic" EI of topologically nonequivalent metal sites.

In spite of the lack of clear "theoretical" proof for the above methodology, we offer an "inductive" justification by showing its performance on several carboranes previously discussed by Gimarc. In these computations we compare our results with the more sophisticated ones reported by Ott and Gimarc[54] using the same experimental or calculated distances (B−B, B−C, B−H, and C−H) and the references therein for all known structures.

1. The EIs computed for $[B_5H_5]^{2-}$ (D_{3h} symmetry; **I**) offer an unambiguous justification for the decreasing order of stability 1,5- > 1,2- > 2,3-$C_2B_3H_5$ discussed in the introduction, given that the 1,5-isomer has a perfect match between the higher EIs in the URF and the location of the more electronegative heteroatoms and the 1,2-isomer matches in only one of the two positions, while in the 2,3-isomer neither carbon occupies a site of lower EI.

2. $[B_6H_6]^{2-}$ has an octahedral geometry. The six vertices of an octahedron are equivalent; therefore, the

(54) Ott, J. J.; Gimarc, B. M. *J. Comput. Chem.* **1986**, *7*, 673.

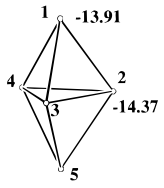

I

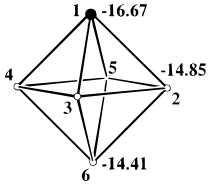

II

EIs of the atoms of the URF must be identical. However, considering the EIs computed for $[CB_5H_6]^-$ (**II**) in this perturbed system, EIs are no longer uniform and we may predict the preferred locations for the second carbon atom. The perturbing carbon atom at position 1 (indicated by • in **II**) induces a higher EI value at position 6. Therefore, 1,6-$C_2B_4H_6$ should be more stable than the 1,2-isomer. This prediction agrees with the experimental report that the 1,2-isomer quantitatively rearranges to the 1,6-isomer on heating at 250 °C.

3. The structures of $[B_7H_7]^{2-}$ and its heteroatomic analogue $[C_2B_5H_7]$ are pentagonal bipyramids. The EIs computed for the URF (**III**) show the equatorial positions to be favored for replacement by more electronegative heteroatoms. For the pentagonal bipyramid there are four possible isomers of $[C_2B_5H_7]$: 1,2, 1,7, 2,3, and 2,4. On the basis of **III** the 2,3- and 2,4-isomers should be the most stable and have comparable stabilities. In order to distinguish between the two, we have introduced a perturbing heteroatom in position 2 (indicated by • in **IV**). The EIs computed for $[CB_6H_7]^-$ (**IV**) show that equatorial positions nonadjacent to the perturbing heteroatom have higher EIs than the adjacent positions, giving the order of stability 2,4 > 2,3 > 1,2 > 1,7. Only the 2,4-isomer has been prepared.

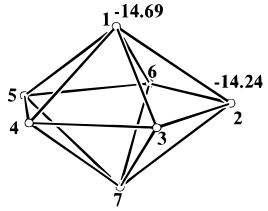

III

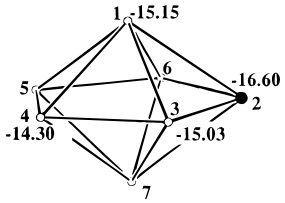

IV

4. $[B_9H_9]^{2-}$ and $[C_2B_7H_9]$ have a tricapped-trigonal-prismatic geometry (D_{3h}). The structure taken as the URF is $[B_9H_9]^{2-}$, shown in **V**, in which there are only two different kinds of sites (1 and 7). The calculated EIs foresee the occupation of site 7 for a carbon atom. We repeated the computation on the $[CB_8H_9]^-$ structure (with C occupying site 7, as shown by • in **VI**): we now have three different sites for the second carbon atom. The highest EI is located in sites 8 and 9 (identical by symmetry); thus, also the second carbon atom will occupy the capped position, as is known experimentally.

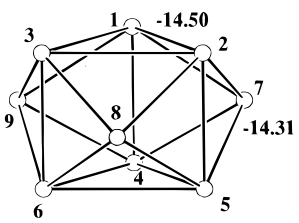

V

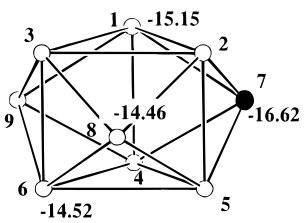

VI

5. The structure for the 10-boron-atom cluster is a bicapped square antiprism (D_{4d} symmetry): the results of computation on $[B_{10}H_{10}]^{2-}$ are shown in **VII**. The two different sites are 1 and 2; the EI of atom 1 is higher, and so the preferred site for carbon is 1. Again we perturb the molecule by introducing a carbon atom in position 1: we now have three different sites (2, 7, and 10). Experimentally all these isomers are known, but the 1,2- and 1,6-species are known only for the dimethyl derivatives. Moreover, according to Gimarc, 1,10 is the most stable isomer. In **VIII** the EIs of $[CB_9H_{10}]^-$ are reported: site 10 has the highest EI and so is the preferred site for the substitution of another carbon atom.

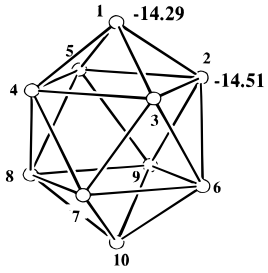

VII

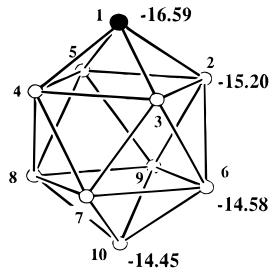

VIII

6. Finally, we considered the icosahedral structure of $[B_{12}H_{12}]^{2-}$. As for the case of octahedral $[B_6H_6]^{2-}$ the high symmetry does not permit us to distinguish any different sites in the homoleptic molecule. Therefore, we must introduce the perturbing carbon atom to generate differentiations of sites. Only three isomers are then possible (1,2 < 1,7 < 1,12, in order of increasing stabilities): in **IX** the EIs of $[CB_{11}H_{12}]^-$ are reported and they show the same order of preference for the substitution of the second carbon atom as observed experimentally.

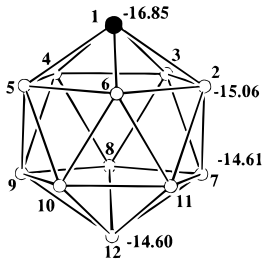

IX

Trigonal-Bipyramidal Metal Carbonyl Clusters

We will use as the M_5L_{15} (76 CVE) URF the $[Rh_5(CO)_{15}]^-$ anion (**A** in Figure 1) with the experimental stereochemistry slightly idealized in order to homogenize the M−C and C−O bond distances of the terminal carbonyl ligands. In contrast, the stereochemistries for the M_5L_{14} (76 CVE), M_5L_{14} (72 CVE), and M_5L_{12} (72 CVE) URFs have been obtained through molecular mechanics computations,[55,56] within C_2 symmetry constraints, on the $[Rh_5(CO)_{14}]^{3-}$, $[Rh_5(CO)_{14}]^+$, and $[Rh_5(CO)_{12}]^{3-}$ species, respectively. The overall stereochemistries of the above URFs are reported in Figure 3; they

(55) Sironi, A. *Inorg. Chem.* **1992**, *31*, 2467.
(56) Sironi, A. *Inorg. Chem.* **1995**, *34*, 1432.

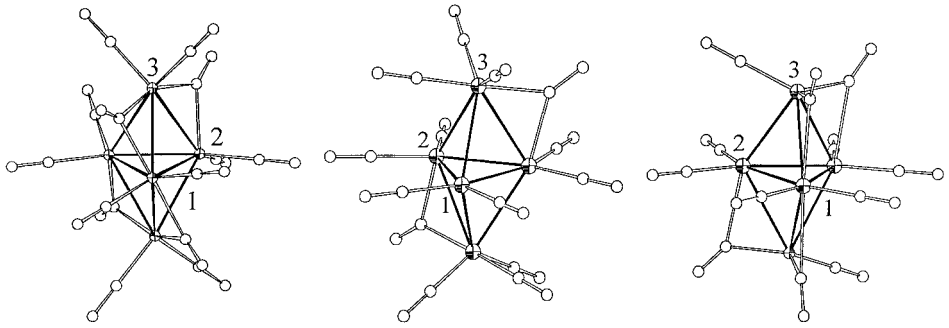

Figure 3. Representations of the molecules used as uniform reference frames (URF). Geometry optimizations of the idealized stereochemistry have been performed with molecular mechanics computations,[55,56] while M−M and M−CO (terminal) distances have been kept fixed to the averaged values observed in all bipyramidal molecules. The M_5L_{15} URF is not shown, because it has the very same stereochemistry as **A** in Figure 1.

all share the same symmetry (C_2), and thus there are only three topologically nonequivalent metal centers, two equatorial (1 and 2) and one apical (3), on each frame.

M_5L_{15}. This is the case for molecules of general formula $[Rh_4M(CO)_{14}L]^{n-}$. There are two known stereogeometries, namely **A**, of C_2 symmetry, found for M = Rh, Co, Ir, L = CO, and $n = 1$ (the same stereochemistry is also present in $[Rh_3Ir_2(CO)_{14}L]^-$), and **B**, of C_s symmetry, found for M = Fe, Ru, Os, L = CO, and $n = 2$, for M = Rh, Ir, L = PPh_3, and $n = 1$, and for M = Rh, L = I, SCN, CH_2CN, and $n = 2$ (see Table 1 and Figure 1). Our aim is to predict both the distribution of metals in the bipyramidal frame and the location of the noncarbonyl ligand when present. The stereochemical changes occurring upon substitution, presently from C_2 to C_s, are due to the variation of the local environment of the "perturbed" metal atom. However, we think, as stated above, that a single computation of the EIs on the M_5L_{15} URF is enough to rationalize site preference. As a matter of fact, as shown in **X**,the apical sites,

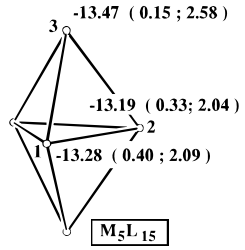

X

having lower EIs, should be preferred by less electronegative metal atoms, i.e. in a frame of group 9 metals by those belonging to group 8, as in $[M_4M'(CO)_{15}]^{2-}$ (M = Rh, Ir and M′ = Fe, Ru, Os) and by (nucleophilic) ligand substitution (having the largest electrophilic character) as in $[M_5(CO)_{14}X]^{n-}$ (M = Rh, Ir and $n = 1$, 2). As discussed previously, Allen's (and our) electronegativities allow us to discriminate between metal atoms belonging to different columns but not between those of different rows (within the same group). Accordingly, we cannot use EIs to foresee the site preference of Co and Ir in a frame of Rh atoms. Following Mingos' approach, we propose to use the criterion of maximum M−M and M−L bonding whenever dealing with metals having similar electronegativities. In **X** we also report, in parentheses, the total M−M and M−CO overlap populations, respectively, computed at each metal site for the M_5L_{15} URF. Site 1 possesses the highest M−M OP; thus, it would be the ideal site for an Ir atom, which, belonging to the third transition row, is estimated to have stronger M−M interactions.[4] In clear contrast with this simple explanation is the fact that $[Rh_4Ir(CO)_{15}]^-$ is a disordered molecule with only 70% of the Ir atoms occupying site 1 and 30% in site 3. Moreover, in the $[Rh_3Ir_2(CO)_{15}]^-$ cluster Ir atoms occupy sites 1 and 3 (not 1 and 2 as could be thought). In this case it is necessary to consider also M−CO interactions. Actually, ligand capabilities are quite uncertain and are difficult to estimate; thus, we may use empirical evidence to predict general trends. In fact, we know that third-row metal atoms generally try to avoid bridging carbonyl ligands. A close look at the C_2 structure clearly shows that equatorial site 1 has two bridging carbonyls and equatorial sites 2 and 2′ have three bridging carbonyls, while apical sites 3 and 3′ have only one bridging carbonyl ligand. Thus, the competition between the best "metallic" site and the best "ligand" site seems to be the cause of the presence of disorder in Ir-substituted M_5L_{15} clusters. In contrast, in $[Rh_4Co(CO)_{15}]^-$ the Co atom is in an apical (3) site, according to the estimated weaker M−M interactions for Co. In Table 5 we also report computed values of total M−M and M−CO OPs for all possible substitutional isomers of $[Rh_5(CO)_{15}]^-$, showing that the observed molecules are those for which we computed the maximum total OP.

Table 5. Total Overlap Populations for Substitutional Isomers of $[Rh_5(CO)_{15}]^-$ [a]

heteroatom site M	total OP M−M		total OP M−Co		total OP M−M + M−CO	
	Co	Ir	Co	Ir	Co	Ir
			Rh_4M			
M(1)	0.63	***0.77***	11.20	***11.74***	11.83	***12.51***
M(2)	0.65	0.76	11.20	11.73	11.85	12.49
M(3)	***0.66***	***0.73***	***11.20***	***11.78***	***11.86***	12.51
			Rh_3Ir_2			
Ir(1), Ir(2)	0.86		12.10		12.96	
Ir(1), Ir(3)	***0.83***		***12.15***		***12.98***	
Ir(2), Ir(2′)	0.84		12.09		12.93	
Ir(2), Ir(3)	0.81		12.14		12.95	
Ir(3), Ir(3′)	***0.79***		***12.19***		***12.98***	

[a] Values in boldface italics refer to the total OPs of the observed molecules.

M_5L_{14}. There are three different structural types, namely **C** and **C′**, of C_2 symmetry, found in $[M_4Pt(CO)_{14}]^{2-}$ (M = Rh, Ir; 76 CVE) and $[M_2M'_3(CO)_{14}]^{n-}$ (M = Fe, M′ = Ir for $n = 1$; M = Ir, M′ = Ru for $n = 2$; 72 CVE), respectively, and **D**, of C_s symmetry, found in $[ReIr_4(CO)_{12}L_2]^-$ (72 CVE). Again, in order to predict both the distribution of metals in the bipyramidal frame and the location of non-carbonyl ligands, we computed the EIs (reported in **XI** and **XII**)on the two M_5L_{14} URFs

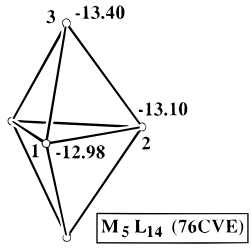

XI

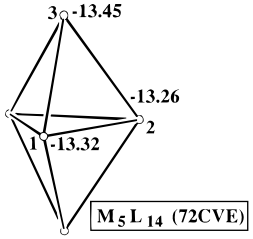

XII

(and the two electron counts). However, since M_5L_{14} homoleptic molecules are (structurally) unknown, we have obtained the two URFs by minimizing with MM[55,56] the steric energies of $[Rh_5(CO)_{14}]^{3-}$ and $[Rh_5(CO)_{14}]^{+}$ within C_2 symmetry constraints. The apical sites have the lowest EI in both the 76- and 72-CVE URFs. The stereochemistries of the $[M_4Pt(CO)_{14}]^{2-}$ (M = Rh, Ir) derivatives are readily rationalized on the basis of the higher electronegativity of the Pt atom (with respect to Rh and Ir), which drives the Pt atom toward the site with the higher EI, namely 1 in **XI**. Upon substitution, there is a large stereochemical transformation which eventually leads to the observed (but *a priori* unknown) stereochemistry (**C** in Figure 1) where the EI at position 1 is definitely the highest; again, what matters here is that the 76-URF (known *a priori*) affords the very same information.

XII allows us to rationalize the stereochemistry of $[Fe_2Ir_3(CO)_{14}]^-$, $[Ir_2Ru_3(CO)_{14}]^{2-}$, and $[ReIr_4(CO)_{12}L_2]^-$, given that the lower electronegativity of the Fe, Ru, and Re atoms (with respect to Ir) drives them toward the sites with the lowest EI, namely 3, 3′, and, when needed, 1. In the $[ReIr_4(CO)_{12}L_2]^-$ anion, the substitution causes a large stereochemical transformation which eventually leads to the observed (but *a priori* unknown) stereochemistry where the EI at position 4 is more definitely the lowest (**D** in Figure 1); however, what matters here is that the 72-CVE URF (known *a priori*) affords the very same information.

In order to rationalize the substitution pattern in $[ReIr_4(CO)_{12}L_2]^-$, we have to compute the EIs for a hypothetical $[ReIr_4(CO)_{14}]^-$ anion. As a matter of fact (see **XIII**), the lowest computed EIs are in positions 3 and 2 (labels as in structure **D** of Figure 1); this, given that two bulky phosphines avoid sharing the same metal atom, implies the observed substitution pattern.

It is worth noting that, as we have done for carboranes, we may choose as the URF for $[Ir_2Ru_3(CO)_{14}]^{2-}$ the (idealized) stereochemistry of $[Ir_3Fe_2(CO)_{14}]^-$, which is experimentally known (**C′**). Indeed, the EIs for the two nonequivalent equatorial positions 1 and 2 (−13.74 and −13.66, respectively) confirm that the third d^8 atom must go in site 1. This choice, which does not require MM computations and allows for a greater similarity

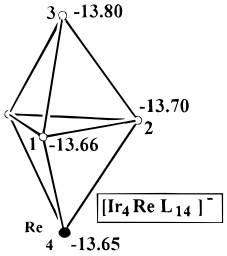

XIII

between the URF and the "final" cluster, can be the general approach for multisubstituted clusters.

M_5L_{12}. There are two similar structural types, namely **E** and **E′**, of C_s symmetry, differing mainly in the presence of three equatorial bridging carbonyls, found in $[Rh_4Pt(CO)_{12}]^{2-}$ and $[Ir_4Pt(CO)_{12}]^{2-}$ (see Table 1 and Figure 1). In order to avoid any bias toward the experimental results, we use as the URF the idealized molecule $[Rh_5(CO)_{12}]^{3-}$ of C_2 symmetry (see above and Figure 3). Unfortunately, the computed EIs are very similar for the three topologically nonequivalent sites (they differ by less than 0.01 eV, and their relative order depends on small stereochemical changes). Thus, even if the Pt atoms are unambiguously located in apical positions in the experimental structures, we cannot discriminate between apical and equatorial sites. We then applied the maximum bond strength criterion, but it also fails in addressing site preference since the computed OP, on the URF, does not clearly discriminate between the different sites.

Conclusions

All EIs reported in this paper have been computed within the EH approximations. In order to assess an internal electronegativity scale for transition metals (which has been later shown to agree well with that developed by Allen) and to allow comparisons of numerical results on moving from left to right and from top to bottom in the periodic table, we determined a homogeneous set of EH parameters.

In this paper, we have proposed, within the frame of TCS, to use EIs instead of charges for addressing "skeletal" site preference. We have shown that EIs behave similarly to charges on "clusters" with a rigid ligand stereochemistry such as carboranes but, when dealing with metal carbonyl clusters and their intriguing ligand mobility, EIs are definitely superior to charges, and they predict that *less* electronegative atoms occupy sites with the *lowest* EIs. Moreover, EIs can also address "ligand" site preference; indeed, the reported examples show that (nucleophilic) ligand substitution preferentially occurs on the *lowest* energy index site of the URF (i.e., that with the *largest* electrophilic character).

The choice of the correct stereochemistry for the URF is at the heart of the method and, when experimental data for the homoleptic $[M_n(CO)_m]^{q-}$ cluster are lacking, molecular mechanics seems to be the correct tool. Note that the experimental (and theoretical) stereochemistries of mixed-metal clusters are intrinsically biased toward the actual metal atom dispositions and cannot be used for the URF. For instance, the EIs computed on $[Rh_5(CO)_{12}]^{3-}$ with the ligand stereochemistry observed in $[Rh_4Pt(CO)_{12}]^{2-}$ (or $[Ir_4Pt(CO)_{12}]^{2-}$), which has an apical Pt atom, clearly suggests an apical location

of the Pt atoms. On the other hand, having built (with MM) the "ideal" stereochemistry for a $[PtRh_4(CO)_{12}]^{2-}$ anion with an equatorial Pt atom and having used *that* ligand geometry for computing the EIs for the $[Rh_5(CO)_{12}]^{3-}$ anion, we obtain a clear preference for an equatorial Pt atom.

Previous attempts to rationalize site preference in metal clusters were mainly concerned with the relative strengths of metal−metal and metal−ligand bonds and substantially disregarded electronegativity differences between different metal atoms. In contrast, we think that the latter are important whenever the actual URF allows for different EIs on different metal sites. In particular, differences in electronegativity have been shown to be important for M_5L_{15} and M_5L_{14} but not for M_5L_{12} bipyramidal metal carbonyl clusters. In the former cases (M_5L_{15} and M_5L_{14}) our results can be summarized by stating that *less* electronegative metal atoms prefer axial sites (since the *lowest* EIs are generally calculated for axial positions). Obviously, whenever the metals have almost the same *atomic* electronegativity (belonging to the same group of the periodic table) or the sites have similar *local* electronegativities EI cannot discriminate between the different sites and Mingos' criterion of maximum bonding (M−M plus M−L) can be applied.

OM960854L